Applied Science and Engineering Progress, Vol. 20, No. 3, 2027, 8318

Research Article

Failure Patterns and Post-Impact Tensile Strength of Bamboo Woven Epoxy Composites with Different Layer Configurations

Khairul Anam*, Bayu Satria Wardhana, Putu Hadi Setyarini, and Adi Wijaya Saputra
Department of Mechanical Engineering, Brawijaya University, Indonesia

* Corresponding author. E-mail: khairul.anam27@ub.ac.id DOI: 10.14416/j.asep.2026.09.009
Received: 3 June 2026; Revised: 10 August 2026; Accepted: 19 August 2026; Published online: 15 September 2026

Abstract
Natural fiber–reinforced composites are increasingly important as sustainable alternatives to synthetic composites, particularly for applications subjected to impact loading. This study investigates the effects of the number of layers and fiber orientation on failure patterns and post-impact tensile strength of black bamboo woven–reinforced epoxy composites. Composite laminates were fabricated using the hand lay-up method with one or two layers and different fiber orientations, including [0°/90°], [+45°/−45°], and hybrid configurations. The specimens were subjected to low-velocity drop-weight impact testing at an impact energy of 15 J, followed by tensile testing to evaluate their residual tensile strength and damage characteristics. The results show that both fiber orientation and the number of layers significantly affect damage distribution and post-impact tensile behavior. Two-layer laminates exhibited approximately 40–50% higher residual tensile strength than single-layer laminates. The [0°/90°/0°/90°] configuration demonstrated the highest load-bearing capacity and the smallest total damage area, with a post-impact strength reduction of only approximately 5%. In contrast, the [+45°/−45°] laminate experienced the greatest strength degradation, approximately 57–58%, due to extensive delamination and shear-dominated failure. In addition, the damage area on the bottom surface was consistently larger than that on the top surface, indicating tensile-dominated failure propagation through the laminate thickness. These findings indicate that increasing the number of layers improves post-impact tensile performance, whereas fiber orientation governs the dominant failure mechanisms and damage propagation behavior. This research provides practical guidance for designing impact-resistant and environmentally friendly composite laminates reinforced with black bamboo woven fibers.

Keywords: Bamboo composite, Failure patterns, Layer configuration, Low-velocity impact, Post-impact tensile strength.

1 Introduction

Natural fiber reinforced polymer composites have been extensively studied as sustainable alternatives to conventional synthetic fiber composites. Their advantages include low density, renewability, biodegradability, and reduced environmental impact during production [1]. These characteristics make natural fibers attractive for applications in automotive components, building materials, and lightweight structures where moderate mechanical performance is sufficient. However, the inherent variability of natural fibers and their sensitivity to processing conditions require careful laminate design to achieve consistent mechanical behavior [2].

Bamboo is one of the most promising natural fibers for composite reinforcement due to its rapid growth, wide availability, and relatively high tensile strength compared with other lignocellulosic fibers [3]. Previous studies have demonstrated that bamboo fibers can provide effective reinforcement when combined with thermoset polymer matrices, particularly epoxy resins. Black bamboo (*Gigantochloa atroviolacea*) has gained attention because of its dense fiber structure and good mechanical performance after alkali treatment, which improves fiber–matrix interfacial bonding [4]. Nevertheless, the mechanical response of bamboo-based composites remains strongly dependent on laminate configuration, including fiber orientation, stacking sequence, and laminate thickness [5].

In service conditions, natural fiber composites may experience impact loading from accidental drops, debris, or handling damage. Low-velocity impact is especially critical for laminated composites, as it can induce internal damage such as matrix cracking, fiber–matrix debonding, and delamination, even when surface damage is not clearly visible [6]. Under low-velocity impact, the laminate response involves localized contact deformation and global bending. The impacted surface is initially subjected to contact compression, whereas laminate deflection generates tensile stresses on the rear surface, which can promote matrix cracking, fiber fracture, and interlaminar separation. Damage may also propagate between adjacent layers through interlaminar shear stresses, thereby reducing the residual load-bearing capacity even when the externally visible damage remains limited. For natural fiber composites, these damage mechanisms are influenced not only by laminate design but also by fiber morphology, fiber–matrix adhesion, and the presence of matrix-rich regions in woven reinforcements [7]. As a result, impact damage tolerance remains a key challenge in the broader application of bamboo-reinforced composites.

Several studies have reported that laminate thickness and fiber orientation affect impact resistance and damage evolution in natural fiber composites. Increasing the number of layers generally enhances energy absorption capacity and stiffness, but also introduces additional interlaminar interfaces that may promote delamination [8]. Previous low-velocity-impact studies on laminated composites have shown that increasing laminate thickness can increase bending stiffness and delay complete penetration; however, the additional interfaces may provide more sites for delamination initiation and propagation. Fiber orientation governs the dominant stress transfer mechanism during impact. Cross-ply configurations such as [0°/90°] tend to concentrate loads along the fiber direction, resulting in more localized damage, whereas angle-ply configurations such as [+45°/−45°] promote shear-dominated deformation and wider delamination areas [9]. These effects are particularly relevant in woven bamboo composites, where fiber crimp and interlacing influence stress redistribution under dynamic loading.

Moreover, residual tensile load after impact is an important parameter for evaluating the structural integrity of natural fiber composites. Impact-induced damage reduces the effective load-bearing cross-section and disrupts stress transfer between fibers and matrix, leading to a noticeable reduction in tensile strength [10]. Although post-impact tensile behavior has been widely investigated in synthetic fiber composites, studies focusing on bamboo woven composites remain limited. Most existing research on bamboo-based composites emphasizes quasi-static tensile or flexural properties, with relatively little attention given to post-impact mechanical performance and associated failure patterns.

Despite the increasing number of studies on natural fiber-reinforced composites, research concerning the post-impact mechanical behavior of woven bamboo epoxy composites remains limited. Most previous studies primarily focused on quasi-static tensile, flexural, or impact properties without evaluating the residual mechanical performance after impact damage [11]. In particular, the influence of stacking sequence and fiber orientation on the relationship between impact-induced failure patterns and post-impact tensile strength has not been comprehensively investigated for black bamboo woven composites [12]. Furthermore, comparative studies between cross-ply, angle-ply, and hybrid laminate configurations under low-velocity impact loading are still scarce [13]. As a result, the dominant failure mechanisms governing residual tensile performance in bamboo woven epoxy laminates are not yet fully understood. Therefore, this study aims to investigate the effect of layer number and fiber orientation on failure patterns and post-impact tensile strength of black bamboo woven epoxy composites subjected to low-velocity impact loading.

The present study aims to examine the effects of layer number and fiber orientation on failure patterns and post-impact tensile strength of black bamboo woven epoxy composites. Laminates with one and two layers and different fiber orientations of [0°/90°], [+45°/−45°], and combined configurations are fabricated using the hand lay-up method. Low-velocity drop weight impact testing is employed to induce controlled damage, followed by tensile testing to assess residual mechanical properties. The results are expected to improve understanding of damage mechanisms in bamboo-based laminates and provide guidance for the design of natural fiber composites with improved impact tolerance.

2 Materials and Methods

2.1 Materials

Black bamboo (*Gigantochloa atroviolacea*) was used as the natural fiber reinforcement in this study. The bamboo was processed into woven mats prior to composite fabrication. To improve fiber–matrix interfacial bonding, the woven bamboo fibers were subjected to an alkali treatment using a 3 wt.% NaOH solution for one hour. A 3 wt.% NaOH treatment for 1 h was selected to partially remove surface waxes and non-cellulosic constituents, increase fiber-surface roughness, and improve epoxy wettability and fiber–matrix adhesion. This relatively mild condition was used to limit excessive cellulose degradation and loss of fiber strength associated with higher alkali concentrations or prolonged treatment. This relatively mild treatment condition was selected to remove surface waxes and part of the non-cellulosic constituents, increase fiber-surface roughness, and improve resin wettability while limiting the cellulose degradation that may occur under more severe alkali treatments. After treatment, the fibers were thoroughly rinsed with distilled water to remove residual alkali and then dried at room temperature until a constant mass was achieved. An epoxy resin system was employed as the polymer matrix due to its good mechanical properties and compatibility with natural fibers. The epoxy resin was mixed with EPH 556 hardener at a resin-to-hardener ratio of 3:1 by volume, following the manufacturer’s recommendations. All materials were used as received after preparation, without further modification.

2.2 Composite fabrication

Composite laminates were fabricated using the hand lay-up method. The woven bamboo was cut to dimensions of 100 mm × 150 mm and arranged according to the designated laminate configurations. Two main variables were considered, including fiber orientation and the number of layers (one layer and two layers). The experimental variables were the number of woven mats and their orientation relative to the subsequent tensile-loading direction. Because each woven mat contained two orthogonal yarn systems, a single mat was denoted [0°/90°] when its principal yarns were aligned with and transverse to the loading direction and [+45°/−45°] when the mat was rotated by 45°. The five configurations were therefore designated [0°/90°], [+45°/−45°], [0°/90°/0°/90°], [+45°/−45°/+45°/−45°], and [0°/90°/+45°/−45°]. The laminate-fabrication procedure is illustrated in Figure 1.

For single-layer laminates, one woven bamboo mat was placed inside a silicone mold, followed by impregnation with the epoxy resin mixture. For two-layer laminates, two woven mats were stacked according to the specified orientation sequence, ensuring proper alignment between layers. Resin impregnation was performed manually to ensure complete wetting of the fibers. After lay-up, the laminates were left to cure at room temperature under atmospheric pressure. The cured laminates were then removed from the mold and trimmed to the required specimen dimensions. The fiber volume fraction was controlled by adjusting the number of woven layers, resulting in approximately 25% fiber volume fraction for single-layer laminates and 50% for two-layer laminates. The final laminate thickness was maintained at approximately 4 mm for all configurations.

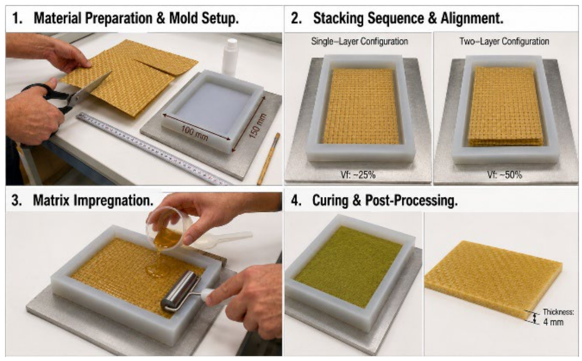

Figure 1: Fabrication procedure and stacking configurations of the woven black-bamboo/epoxy laminates.

Low-velocity impact testing was conducted using a drop-weight impact testing machine (see Figure 2) following the general principles of ASTM D7136. Rectangular specimens with dimensions of 100 mm × 150 mm were clamped using a fixture to ensure consistent boundary conditions during impact loading. A hemispherical steel impactor with a diameter of 15 mm was used to strike the center of the specimen. The impact energy was set at 15 J by adjusting the drop height and impactor mass. During testing, the impactor was allowed to freely fall onto the specimen surface to generate controlled impact damage. The impact response was recorded in terms of visible damage characteristics, including matrix cracking, fiber fracture, delamination, and rear-surface failure patterns. After testing, all specimens were visually inspected from both the impacted (front) and non-impacted (rear) surfaces. Photographic documentation was carried out immediately after impact testing using a digital camera under consistent lighting conditions to facilitate subsequent damage area analysis.

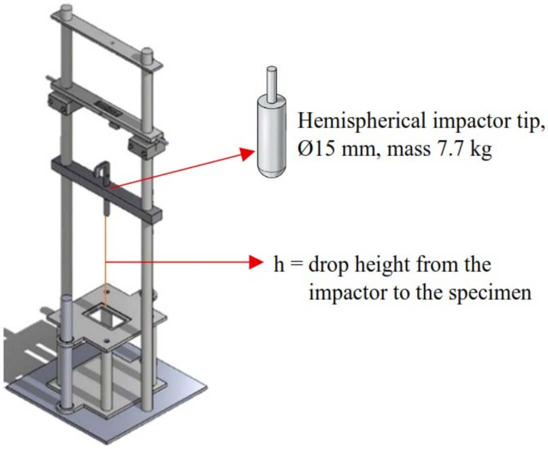

Figure 2: Schematic illustration of the low-velocity drop-weight impact setup, showing the 7.7 kg impactor, effective drop height, clamped specimen, and central impact location.

2.3 Impact testing

Low-velocity impact testing was conducted using a drop-weight impact testing machine (Figure 2) with specimen preparation and impact positioning based on ASTM D7136. Rectangular specimens measuring 100 mm × 150 mm with a thickness of 4 mm were clamped in the test fixture to maintain consistent boundary conditions. Before testing, each specimen was visually inspected to exclude specimens with pre-existing surface cracks. A 7.7 kg steel impactor with a 15 mm hemispherical tip was positioned over the center of the specimen. The nominal impact energy was fixed at 15 J for comparative damage assessment. From a gravitational potential energy equation, an effective drop height of 0.208 m was required, corresponding to a theoretical impact velocity of approximately 2.02 m s. Because the impactor was 0.11 m long, the release position on the apparatus was set at 0.318 m above the specimen reference level. The impactor was released manually and allowed to fall freely onto the center of the clamped specimen. The same incident energy was applied to all configurations to provide a common loading condition. The selected 15 J condition should therefore be interpreted as a fixed comparative impact level rather than an equivalent damage-severity level for every laminate**.** After impact, all specimens were visually inspected from both the impacted and rear surfaces. Photographs were captured immediately after testing under consistent lighting, camera-distance, and specimen-positioning conditions for subsequent surface-damage analysis. Three nominally identical specimens were prepared for each laminate configuration.

2.4 Surface damage area measurement

Damage area quantification was performed using digital image analysis with ImageJ software. After impact testing, photographs of the impacted (front) and non-impacted (rear) surfaces of each specimen were captured using a digital camera under consistent lighting and fixed-distance conditions to ensure measurement consistency. The known specimen dimensions were used to calibrate the pixel-to-length scale before area measurement. The acquired images were imported into ImageJ for damage-area evaluation. Matrix cracking was operationally identified as narrow, visually continuous surface fissures without observable lifting or separation of the woven layer. Surface-visible delamination-like damage was identified as a broader region showing whitening, local lifting, separation, or loss of continuity between the reinforcement and surrounding matrix. Visible discontinuity or severing of bamboo yarns was classified as fiber breakage. The identified regions were manually outlined using the thresholding and area-selection tools and converted into binary images to facilitate area calculation. Overlapping regions were classified according to the dominant visible feature to avoid double counting. Matrix-cracking and surface-visible delamination-like areas were measured separately in mm² on each specimen surface.

2.5 Pristine and post-impact tensile testing

Tensile tests were performed on pristine and impacted specimens to compare their tensile load-bearing capacities. The tests were conducted using a KEJIAN universal testing machine under displacement-controlled loading; the machine had a stated load-measurement accuracy of ±0.5%. The 100 mm × 150 mm impacted panels were positioned directly between the grips, with the impact site located within the loaded region. ASTM D7136 was used only for the impact-specimen geometry and does not constitute a post-impact tensile standard. Because the impacted panels were not machined into a standard tensile-coupon geometry and the effective load-bearing cross-sectional area could not be determined reliably after localized impact damage, the test was treated as a comparative residual-load assessment rather than a standardized tensile-strength measurement. The load–displacement response was recorded for each specimen, and the maximum tensile load was used to determine the residual load-bearing capacity. Accordingly, the mechanical results are reported in newtons rather than as tensile strength in megapascals, and the initial load–displacement slope is interpreted as effective structural stiffness rather than an intrinsic elastic modulus**.** The tensile behavior of impacted specimens was compared with that of pristine specimens and among laminate configurations to assess the influence of mat number and fiber orientation on residual mechanical performance.

2.6 Failure analysis

Failure patterns resulting from impact and subsequent tensile loading were analyzed macroscopically by visual examination of the impacted and rear surfaces. Damage features such as matrix cracking, surface-visible interfacial separation, fiber breakage, and fiber pull-out were identified. The damage distribution was interpreted in terms of local indentation, impact-induced bending, rear-face tensile stress, matrix-dominated shear deformation, yarn breakage, and interfacial separation. Particular attention was given to the strain incompatibility between adjacent [0°/90°] and [+45°/−45°] mats in the hybrid laminate because their different principal deformation directions can generate interlaminar shear and normal stresses that promote crack deflection, branching, and interface separation. The extent and distribution of damage were compared among different laminate configurations and related quantitatively to the retained maximum tensile load.

3 Results and Discussion

3.1 Failure patterns after impact

Failure patterns of woven black-bamboo/epoxy composites observed on the impacted and rear surfaces for the [0°/90°], [+45°/−45°], [0°/90°/0°/90°], [+45°/−45°/+45°/−45°], and [0°/90°/+45°/−45°] configurations are shown in Figure 3. On the impacted surface, all specimens exhibit localized indentation at the impact center, accompanied by surface-visible matrix cracks and yarn breakage. However, the extent, direction, and distribution of these features vary with laminate configuration. The [0°/90°] configuration shows relatively symmetric and localized damage around the impact point, consistent with load redistribution along its two orthogonal yarn directions. In contrast, the [+45°/−45°] configuration presents a rotated and more irregular crack pattern aligned approximately with the diagonal yarn directions. This pattern indicates a greater contribution from matrix-dominated shear deformation and yarn rotation. The hybrid [0°/90°/+45°/−45°] laminate exhibits a less uniform crack network because its adjacent woven mats have

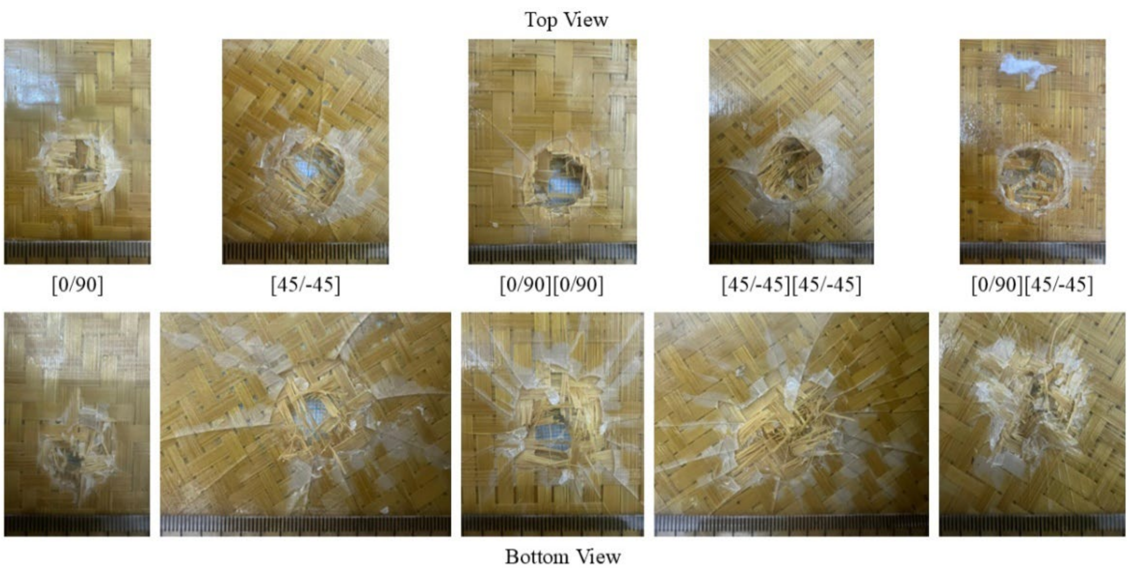

Figure 3: Surface-visible failure patterns of woven black-bamboo/epoxy laminates after 15 J low-velocity impact loading for different laminate configurations, as observed on the impacted and rear surfaces.

different principal stiffness and deformation directions. On the rear surface, the visible damage is more extensive than that on the impacted surface across the tested configurations. Petal-like cracking, surface-visible separation, yarn breakage, and fiber pull-out are observed, indicating that flexural deformation generated tensile stresses on the rear face. The repeated angle-ply configuration, [+45°/−45°/+45°/−45°], shows broader radial crack propagation than the repeated cross-ply configuration, whereas the hybrid laminate demonstrates crack branching and deflection associated with the interaction between the dissimilar mat orientations. Because the specimens were opaque and no internal-damage inspection was performed, the visible separation regions are interpreted as surface-visible delamination-like damage rather than direct measurements of subsurface delamination.

The observed failure patterns indicate that laminate configuration influences stress redistribution and the direction of crack propagation in woven bamboo/epoxy composites under impact loading. The relatively confined damage in the [0°/90°] configuration suggests that orthogonal yarn alignment distributes the local impact load along the principal material directions and restricts lateral crack extension [14], [15]. This is consistent with findings that support the effectiveness of a cross-ply arrangement, as it allows for better energy dissipation across the laminate layers, mitigating localized failure [16]. Conversely, angle-ply laminates of [0°/90°/45°/−45°] are more susceptible to shear-driven delamination due to fiber orientation at ±45°, which promotes sliding and interlaminar separation under impact-induced shear stresses [17], [18]. Research findings indicate a tendency for extensive damage on the bottom surfaces, confirming that the tensile stresses arising from the stress wave transmission through the laminate thickness govern final failure. Such observations are corroborated in studies assessing the initiation and progression of delamination under similar load conditions [19].

Moreover, the [0°/90°/+45°/−45°] hybrid configuration combines mats with different principal stiffness and deformation directions, producing strain incompatibility at the interface during impact-induced bending. The resulting interlaminar shear and normal stresses can cause an approaching matrix crack to deflect along the interface, branch into multiple paths, or propagate into the adjacent mat in a different direction, thereby producing a more complex crack network [20]. This complexity arises from the competing mechanisms of crack initiation and propagation influenced by varying stacking sequences that introduce directional weaknesses [21], [22]. A complex crack network should not automatically be interpreted as lower structural integrity: crack deflection may dissipate fracture energy, whereas extended interface separation can reduce load transfer during subsequent tensile loading. Its net effect must therefore be evaluated together with the measured damage area and retained maximum tensile load. Overall, it is demonstrated that while woven bamboo composites can absorb impact energy, their post-impact damage tolerance is highly dependent on layer configuration, which directly affects delamination resistance, crack propagation control, and ultimately residual tensile performance [23]. Utilization of careful design in the stacking sequence and configuration can enhance the structural resilience of bamboo woven epoxy composites, contributing to their potential applications in various engineering fields [24].

3.2 Surface damage area

Figure 4 presents (a) matrix cracking area, (b) delamination area, and (c) total damage area for different laminate configurations. In Figures 4(a) and

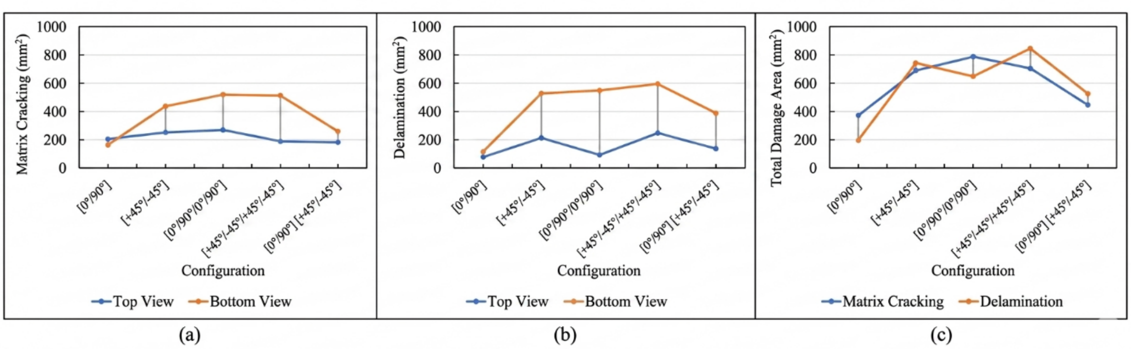

Figure 4: Quantitative comparison of impact-induced damage areas for different laminate configurations (a) matrix cracking area from top and bottom views, (b) delamination area from top and bottom views, and (c) total damage area.

(b), the bottom view consistently exhibits larger damage areas than the top view across all configurations, indicating more severe tensile-dominated failure on the rear surface. For matrix cracking, the highest damage is observed in the [+45°/−45°/+45°/−45°] configuration on the bottom surface, while the [0°/90°] configuration shows the lowest cracking area. A similar trend appears in delamination, where angle-ply and repeated angle-ply laminates demonstrate higher delamination areas compared to cross-ply laminates. Figure 4(c) shows that total damage area (combined matrix cracking and delamination) reaches its maximum in the [+45°/−45°/+45°/−45°] configuration, followed by hybrid stacking [0°/90°/0°/90°] and [+45°/−45°]. The [0°/90°] laminate consistently presents the smallest total damage area, indicating better resistance to impact-induced failure.

The observed trends indicate that laminate configuration influences both the magnitude and spatial distribution of surface-visible impact damage in woven bamboo/epoxy composites. The relatively low impacted-surface separation area of the [0°/90°] laminate suggests that orthogonal yarn orientation promotes load redistribution along the principal material directions and restricts the lateral extension of the initially damaged region [25]. This observation aligns with previous research highlighting the advantages of cross-ply configurations in improving impact resistance [26]. In contrast, the [+45°/−45°] and [+45°/−45°/+45°/−45°] laminates transfer a greater proportion of the impact-induced deformation through matrix shear, yarn rotation, and interfacial sliding. These mechanisms can distribute surface cracking over a wider region while increasing susceptibility to interface separation along the inclined yarn directions [27].

The larger damage recorded on the bottom surfaces confirms that tensile stress waves transmitted through the laminate thickness govern the dominant failure mechanism, underscoring the importance of laminate thickness and orientation in managing impact forces [24]. The high total damage area in repeated angle-ply laminates implies that shear-dominated failure mechanisms contribute more critically to structural degradation than normal stress components, as indicated by the predominant delamination failures observed in angle-ply configurations [5]. Nevertheless, damage area alone does not fully determine residual mechanical performance. The cross-ply laminates retain direct 0° yarn load paths during subsequent tensile loading, whereas the angle-ply laminates depend more strongly on matrix- and interface-mediated shear transfer. Consequently, impact damage affecting the matrix and interface can produce a disproportionately large reduction in the residual maximum tensile load of the angle-ply configuration, even when differences in visible damage area are comparatively moderate. These findings highlight that cross-ply configurations may offer better impact tolerance and potentially higher post-impact tensile strength compared to angle-ply dominated laminates, supporting the notion that strategic design of stacking sequences can enhance the mechanical performance and durability of bamboo woven epoxy composites [28], [29].

3.3 Load-displacement curve

Figure 5 presents the load–displacement curves of specimens in (a) the pristine condition and (b) after 15 J impact loading. In Figure 5(a), all reinforced laminates exhibit higher maximum tensile loads than the unreinforced epoxy specimen. The [0°/90°/0°/90°] and [0°/90°/+45°/−45°] configurations achieve the highest peak loads, exceeding 600 N, which reflects their greater tensile load-bearing capacity. Their relatively steep initial load–displacement slopes also indicate higher effective structural stiffness than the single-layer configurations. The [+45°/−45°/+45°/−45°] laminate exhibits a comparatively steep initial slope followed by an abrupt post-peak load reduction, indicating rapid loss of its remaining load path after the maximum load is reached. Meanwhile, the single-layer angle-ply [+45°/−45°] configuration records a lower peak load than the cross-ply and hybrid laminates. The larger crosshead displacement observed for some configurations should not be interpreted directly as material ductility because the measured displacement includes specimen, grip, and testing-machine compliance. In Figure 5(b), all configurations show lower maximum loads after impact than in their corresponding pristine conditions. The reduction is most pronounced in the [+45°/−45°] laminate, which exhibits the lowest residual maximum tensile load. The cross-ply-dominated and hybrid laminates retain comparatively higher load-bearing capacities, indicating more effective redistribution of the tensile load around the impact-damaged region. Because the curves present load against crosshead displacement,

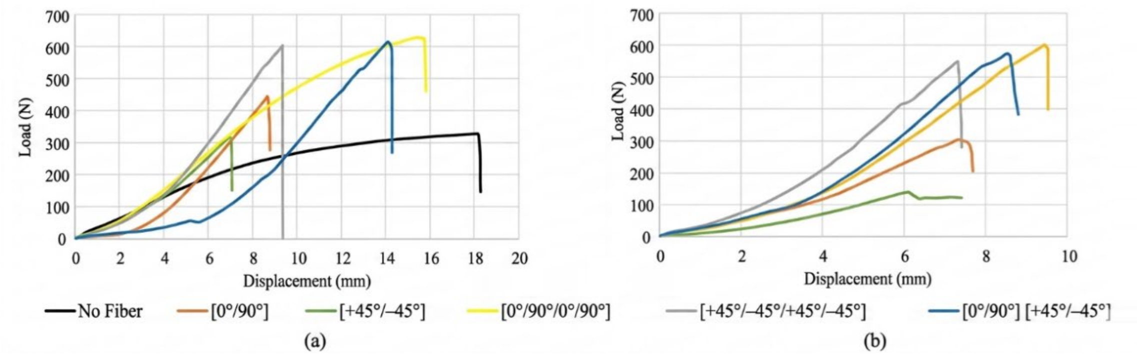

Figure 5: Load–displacement responses of woven black-bamboo/epoxy laminates in (a) the pristine condition and (b) after 15 J low-velocity impact loading for the different laminate configurations.

the measured maximum response is reported as residual load-bearing capacity in newtons rather than tensile strength in megapascals.

The comparison between Figures 5(a) and 5(b) demonstrates that prior impact loading reduces the effective structural stiffness, maximum tensile load, and displacement to failure of the tested laminates, although the magnitude of the reduction depends on laminate configuration. In the pristine condition, cross-ply and hybrid stacking sequences provide more efficient stress transfer along principal fiber directions, resulting in higher stiffness, strength, and energy absorption [30]. These characteristics are critical in ensuring that the composite maintains its structural integrity under various loading conditions. However, after impact, internal damage such as matrix cracking, delamination, and fiber breakage reduces the laminate’s ability to effectively redistribute tensile stresses [31]. This damage is manifested in the curves as a reduced initial slope, a lower peak load, an earlier onset of nonlinearity, or a more abrupt post-peak load loss.

The more pronounced maximum-load reduction observed in the [+45°/−45°] configuration indicates that the single-layer angle-ply laminate is particularly vulnerable to impact-induced matrix and interfacial shear damage. Under subsequent tensile loading, neither principal yarn family is aligned directly with the loading axis; therefore, load transfer depends strongly on matrix shear, yarn rotation, and fiber–matrix interfacial continuity. Impact-induced cracking and surface-visible separation disrupt these mechanisms and promote earlier localization of shear deformation and interface failure [32]. Indeed, research has indicated that angle-ply configurations are generally less effective in sustaining post-impact loads when compared to their cross-ply counterparts, primarily due to the shear-dominated failure mechanisms they promote [33]. Although hybrid configurations still maintain comparatively better residual strength, the overall decrease in slope and peak load in Figure (b) indicates stiffness degradation and premature failure due to internal defects [34]. These findings demonstrate that stacking sequence not only influences initial tensile properties but also governs post-impact residual performance and structural damage tolerance, reiterating the need for careful consideration in the design of composite materials [35].

3.4 Load bearing capacity

Figure 6 presents the load-bearing capacity of bamboo woven epoxy composite laminates under pristine conditions and after-impact conditions for various stacking configurations. In the pristine condition, all reinforced laminates show higher maximum loads compared to the no-fiber specimen. The [0°/90°/0°/90°] configuration exhibits the highest load-bearing capacity, followed by [0°/90°/+45°/−45°] and [+45°/−45°/+45°/−45°]. The single-layer [0°/90°] laminate demonstrates moderate strength, while the [+45°/−45°] configuration records the lowest maximum load among the reinforced specimens. After impact, all configurations experience a noticeable reduction in maximum tensile load. The reduction is most pronounced in the [+45°/−45°] laminate, whereas multilayer and hybrid laminates maintain relatively high residual strength compared to single-orientation laminates.

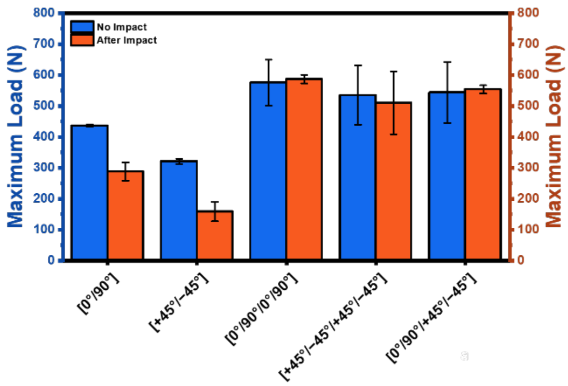

Figure 6: Load-bearing capacity of bamboo woven epoxy composite laminates in pristine condition and after-impact conditions for various stacking configurations.

The comparison between pristine and impacted conditions indicates that stacking sequence plays a crucial role in post-impact strength retention. The [+45°/−45°] laminate exhibits the largest strength degradation, with a reduction of approximately 57–58%, indicating high susceptibility to shear-induced damage and interlaminar failure [36]. This reduction can be explained mechanically by the absence of a principal yarn family aligned directly with the tensile-loading direction. Axial loading of the ±45° yarns depends on yarn rotation, matrix shear, and fiber–matrix interfacial transfer. Impact-induced matrix cracking and surface-visible interface separation consequently degrade the same mechanisms required to carry the subsequent tensile load, leading to earlier shear localization and failure. In contrast, the [0°/90°] configuration experiences a moderate decrease of about 33%, suggesting better axial load transfer while still demonstrating limited damage tolerance in single-layer forms [37]. The 0° yarns provide a more direct axial load path and allow part of the applied load to bypass the locally damaged region. However, because this configuration contains only one woven mat and a larger matrix-rich proportion, its capacity for load redistribution remains more limited than that of the two-mat configuration.

The multi-layer configurations exhibit smaller maximum-load reductions: approximately 5% for [0°/90°/0°/90°], 8% for [+45°/−45°/+45°/−45°], and 7% for the hybrid [0°/90°/+45°/−45°] laminate. These values correspond to approximate load retentions of 95%, 92%, and 93%, respectively. The high retention of the repeated cross-ply laminate is attributed to the continuity and redundancy of the 0° yarn load paths: when impact damage locally interrupts part of the reinforcement, the remaining aligned yarns and the second woven mat can redistribute the tensile load around the damaged region [38].

The repeated angle-ply laminate also retains a comparatively high maximum load despite its extensive surface-visible damage. This result indicates that visible damage area alone does not determine residual capacity; the additional woven mat and higher nominal reinforcement content provide redundant load-transfer paths even though matrix shear and interface separation remain extensive. The hybrid laminate combines direct axial load transfer through its 0° yarns with load redistribution through the ±45° mat. However, directional-stiffness and strain mismatch at the dissimilar interface can promote crack deflection and surface separation. The lower percentage reductions should not be interpreted as direct evidence of better interlayer bonding or greater impact-energy absorption because neither interfacial bond strength nor an instrumented impact-energy history was measured. Therefore, the two-layer cross-ply and hybrid configurations demonstrate better post-impact maximum-load retention under the present 15 J test condition than the single-layer angle-ply laminate [28]. Nevertheless, mat number and nominal fiber content increased simultaneously; thus, the improved retention cannot be attributed to stacking sequence or layer interaction alone.

4 Conclusion

This study investigated the effects of woven-mat number and orientation on surface-visible impact damage and residual tensile load-bearing capacity of black-bamboo woven/epoxy composites subjected to a 15 J impact. The single-layer [+45°/−45°] laminate exhibited the greatest maximum-load reduction of approximately 57–58%, whereas the single-layer [0°/90°] laminate showed a 33% reduction. The two-layer [0°/90°/0°/90°], [+45°/−45°/+45°/−45°], and hybrid [0°/90°/+45°/−45°] laminates showed reductions of approximately 5%, 8%, and 7%, respectively. The repeated angle-ply laminate exhibited the largest surface-visible separation area, increasing from 248.558 mm² on the impacted surface to 596.441 mm² on the rear surface. Cross-ply configurations maintained more effective axial load paths through the 0° yarns, whereas angle-ply configurations were governed by matrix shear, yarn rotation, and interfacial separation. Increasing the number of woven mats improved load redistribution but simultaneously increased the nominal reinforcement fraction and number of interfaces. Because the study was limited to surface-based damage measurements, one- and two-mat laminates, and a single impact energy, future studies should independently control thickness and fiber fraction, examine additional layers and impact energies, and employ internal-damage characterization and standardized tensile testing.

Acknowledgments

The authors would like to acknowledge that this research was supported by the Directorate of Research and Community Service, Universitas Brawijaya, through the Competitive Research Grant – Fundamental Research Scheme (Penelitian Dasar Madya), under Contract No. 00738.54/UN10.A0501/B/PT.01.03.2/2025.

Author Contributions

KA planned the research framework, initiated the project, supervised the overall study, and contributed to data analysis and interpretation; BSW and AWS conducted the experimental work and data acquisition; PHS contributed to methodology development and data validation; PKAVK and HEP provided scientific input, critical review, and technical discussion. The manuscript was written through the contribution of all authors. All authors discussed the results, reviewed, and approved the final version of the manuscript.

Conflicts of Interest

The authors declare no conflict of interest.

Declaration of generative AI and AI-assisted technologies in the writing process

During the preparation of this work the author(s) used [ChatGPT and SciSpace] in order to [enhance the language and readability of the manuscript, find out and relate causal reasons]. After using this tool/service, the author(s) reviewed and edited the content as needed and take(s) full responsibility for the content of the publication.

References

[1] A. M. Radzi et al., "Bamboo-fiber-reinforced thermoset and thermoplastic polymer composites: A review of properties, fabrication, and potential applications," *Polymers (Basel)*, vol. 14, no. 7, pp. 1387, Art. no. 1387, 2022, doi: 10.3390/polym14071387.

[2] N. M. Norizan et al., "Mechanical performance evaluation of bamboo fibre reinforced polymer composites and its applications: A review," *Functional Composites and Structures*, vol. 4, no. 1, Art. no. 15009, 2022, doi: 10.1088/2631-6331/ac5b1a.

[3] M. Haris, D. Laila, E. Zainudin, F. Mustapha, R. Zahari, and Z. Halim, "Preliminary review of biocomposites materials for aircraft radome application," *Key Engineering Materials*, vol. 471–472, pp. 563–567, 2011, doi: 10.4028/www.scientific.net/kem.471-472.563.

[4] B. Oliver, Q. Dong, M. Ramezani, M. Cantó, and S. Caballero, "Tribological performance of bamboo fabric reinforced epoxy composites," *Macromolecular Materials and Engineering*, vol. 308, no. 9, Art. no. 2300077, 2023, doi: 10.1002/mame.202300077.

[5] A. Suhaimi, A. Ali, K. Rassiah, and K. K.Z, "Impact behaviour of laminated bamboo, E-glass and hybrid bamboo/E-glass fibre composites," *International Journal of Integrated Engineering*, vol. 14, no. 8, pp. 92–100, 2022, doi: 10.30880/ijie.2022.14.08.012.

[6] S. Mahesh et al., "Influence of incident energy on sisal/epoxy composite subjected to low velocity impact and damage characterization using ultrasonic C-scan," *Applied Science and Engineering Progress*, vol. 15, no. 1, Art. no. 5220, 2022, doi: 10.14416/j.asep.2021.07.005.

[7] M. Rajput, M. Burman, F. Forsberg, and S. Hallström, "Experimental and numerical study of the response to various impact energy levels for composite sandwich plates with different face thicknesses," *Journal of Sandwich Structures & Materials*, vol. 21, no. 5, pp. 1654–1682, 2019, doi: 10.1177/1099636219837133.

[8] L. F. Ng, M. Y. Yahya, C. Muthukumar, J. Parameswaranpillai, H. Y. Leong, and S. M. S. A. S. Hamzah, "Drop-weight impact responses of kenaf fibre-reinforced composite-metal laminates: Effect of chemical treatment and fibre

composition," *Applied Science and Engineering Progress*, vol. 17, no. 4, Art. no. 7082, Oct. 2024, doi: 10.14416/j.asep.2023.11.006.

[9] B. Elamvazhudi and S. Gopalakannan, "Long-term behavior of nanoclay/TiO_2 nanoparticles modified carbon/glass fiber–reinforced hybrid composites," *Journal of Testing and Evaluation*, vol. 51, no. 4, pp. 2468–2489, 2023, doi: 10.1520/JTE20220452.

[10] N. Z. M. Zuhudi, K. Jayaraman, and R. J. T. Lin, "Mechanical, thermal and instrumented impact properties of bamboo fabric-reinforced polypropylene composites," *Polymers and Polymer Composites*, vol. 24, no. 9, pp. 755–766, Nov. 2016, doi: 10.1177/096739111602400912.

[11] D. K. Mohapatra, C. R. Deo, P. Mishra, K. K. Ekka, and C. Mishra, "Mechanical characterization of kenaf/glass fibre hybrid composite laminates: An experimental and numerical approach," in *Proceedings of the Institution of Mechanical Engineers Part E Journal of Process Mechanical Engineering*, vol. 237, no. 6, pp. 2440–2448, 2023, doi: 10.1177/09544089221136813.

[12] Y. Munde, A. Panigrahi, G. Chandekar, A. Shinde, and I. Siva, "Identifying the influence of stacking sequence on mechanical and vibration properties of bamboo/glass-epoxy composites," *Macromolecular Symposia*, 2023, doi: 10.1002/masy.202200170.

[13] M. K. Meravi and V. Panchore, "Fiber alignment's effect on the properties of hybrid glass/flax fiber-reinforced epoxy composite laminates" *Polymers for Advanced Technologies*, vol. 35, Art. no. e6618, 2024, doi: 10.1002/pat.6618.

[14] G. Murri and E. Guynn, "Analysis of delamination growth from matrix cracks in laminates subjected to bending loads," in *Composite Materials: Fatigue and Fracture*, pp. 322–339, 1988, doi: 10.1520/STP26143S.

[15] H. Ullah, A. Harland, and V. Silberschmidt, "Damage in woven CFRP laminates under impact loading," *EPJ Web of Conferences*, vol. 26, Art. no. 04004, 2012, doi: 10.1051/epjconf/20122604004.

[16] C. Rubio-González, E. José-Trujillo, F. Chávez, and A. Ruíz, "Low velocity impact response of composites and fiber metal laminates with open holes," *Journal of Composite Materials*, vol. 51, no. 6, pp. 797–810, 2016, doi: 10.1177/0021998316653817.

[17] Y. Hirano and A. Todoroki, "Damage identification of woven graphite/epoxy composite beams using the electrical resistance change method," *Journal of Intelligent Material Systems and Structures*, vol. 18, no. 3, pp. 253–263, 2007, doi: 10.1177/1045389x06065467.

[18] N. Keršienė and A. Žiliukas, "Interlaminar and intralaminar damage mechanisms of impact resistant aircraft materials under low-energy impact," *Aviation*, vol. 10, no. 3, pp. 3–8, 2006, doi: 10.3846/16487788.2006.9635933.

[19] J. Lee and J. Kim, "Impact response of carbon fibre fabric/thermoset-thermo-plastic combined polymer composites," *Advanced Composites Letters*, vol. 26, no. 3, 2017, doi: 10.1177/096369351702600304.

[20] R. Rathanasamy, R. Asokan, C. Santulli, A. Pavlović, and C. Fragassa, "The effect of fibre bridging on mode I interlaminar fracture toughness of carbon-aramid/epoxy intra-ply hybrid laminates," *Tribology in Industry*, vol. 41, no. 1, pp. 64–75, 2019, doi: 10.24874/ti.2019.41.01.08.

[21] B. Vieille, V. Casado, and C. Bouvet, "About the impact behavior of woven-ply carbon fiber-reinforced thermoplastic- and thermosetting-composites: A comparative study," *Composite Structures*, vol. 101, pp. 9–21, 2013, doi: 10.1016/j.compstruct.2013.01.025.

[22] A. Pegoretti, I. Cristelli, and C. Migliaresi, "Experimental optimization of the impact energy absorption of epoxy–carbon laminates through controlled delamination," *Composites Science and Technology*, vol. 68, no. 13, pp. 2653–2662, 2008, doi: 10.1016/j.compscitech.2008.04.036.

[23] S. Jäger, A. Pickett, and P. Middendorf, "A discrete model for simulation of composites plate impact including coupled intra- and inter-ply failure," *Applied Composite Materials*, vol. 23, no. 2, pp. 179–195, 2015, doi: 10.1007/s10443-015-9455-2.

[24] A. Ali, K. Rassiah, and M. Ahmad, "The effect of stacking sequence of woven bamboo on mechanical behavior of fiber-reinforced composites," *Journal of Southwest Jiaotong*

University, vol. 56, no. 2, pp. 591–604, 2021, doi: 10.35741/issn.0258-2724.56.2.48.

[25] E. Randjbaran, D. Majid, M. Sultan, N. Mazlan, and R. Zahari, "Tensile strength of reinforced laminates after oblique ballistic impact: An experimental study," *Journal of Industrial Textiles*, vol. 52, 2022, doi: 10.1177/15280837221121943.

[26] V. Anuse, K. Shankar, V. Ramachandran, and S. Ha, "LVI and CAI analysis of woven carbon fiber reinforced composite laminates with different stacking sequence," *Key Engineering Materials*, vol. 969, pp. 93–100, 2023, doi: 10.4028/p-n2mcug.

[27] H. Dalfi, "Improving the mechanical performance and impact damage tolerance of glass composite laminates via multi-scales of hybridisation," in *Proceedings of the Institution of Mechanical Engineers, Part L: Journal of Materials: Design and Applications*, vol. 236, no. 12, pp. 2339–2356, 2022, doi: 10.1177/14644207211073026.

[28] J. Cai, J. Zeng, F. Ye, and W. Kong, "Analysis of CFRP laminates properties under different layup structure using finite element analysis," *Engineering, Materials Science*, vol. 18, pp. 249–254, 2021, doi: 10.21741/9781644901311-30.

[29] A. Rogani, P. Navarro, S. Marguet, and J. Ferrero, "Study of post-impact behaviour of thin carbon/epoxy laminates subject to fatigue tensile loading, *International Journal of Fatigue*, vol. 148, pp. 106134, 2021, doi: 10.1016/j.ijfatigue.2020.106134.

[30] H. Li, K. Liu, Z. Tao, Z. Yu, L. Ye, and W. Xiao, "Effect of stacking sequence on the double-point low velocity impact response and compression-after-impact behavior of glass fiber-reinforced composite laminates," *Polymer Composites*, vol. 46, no. 9, pp. 8474–8489, 2025, doi: 10.1002/pc.29504.

[31] H. Mei, D. Han, S. Farhan, L. Cheng, H. Xu, and Y. Liu, "Impact behavior of different cross-ply laminated carbon fiber-reinforced silicon carbide composites under the low velocity," *Journal of Composite Materials*, vol. 50, no. 8, pp. 1137–1142, 2015, doi: 10.1177/0021998315588775.

[32] M. K. R. Hashim et al., "Effects of Ply Orientations and Stacking Sequences on Impact Response of Pineapple Leaf Fibre (PALF)/Carbon Hybrid Laminate Composites," *Materials*, vol. 15, no. 17, pp. 6121, 2022, doi: 10.3390/ma15176121.

[33] M. Azeem et al., "Macroscale assessment of low-velocity impact on hybrid composite laminates," *Materwiss. Werksttech.*, vol. 52, no. 10, pp. 1101–1111, 2021, doi: 10.1002/mawe.202000325.

[34] N. Sharma and K. Singh, "Transverse fatigue behavior analysis of symmetric and asymmetric glass fiber-reinforced laminates," *Polymer Composites*, vol. 44, no. 5, pp. 2871–2886, 2023, doi: 10.1002/pc.27287.

[35] G. Dress, M. Woldemariam, and D. Redda, "Influence of fiber orientation on impact resistance behavior of woven sisal fiber reinforced polyester composite," *Advances in Materials Science and Engineering*, vol. 2021, no. 1, 2021, doi: 10.1155/2021/6669600.

[36] M. Pires and V. Chalivendra, "In-situ damage sensing in intra-ply glass/carbon laminate composites under interlaminar shear loading," *Journal of Composite Materials*, vol. 56, no. 2, pp. 213–222, 2021, doi: 10.1177/00219983211049291.

[37] S. Turaka and A. Bandaru, "Enhancement in mechanical properties of glass/epoxy composites by a hybrid combination of multi-walled carbon nanotubes and graphene nanoparticles," *Polymers (Basel).*, vol. 15, no. 5, p. 1189, 2023, doi: 10.3390/polym15051189.

[38] V. Babu, V. Arumugam, and C. Santulli, "Damage monitoring of glass/epoxy-curved laminates with different stacking sequences using acoustic emission," *Structural Health Monitoring*, vol. 24, no. 6, pp. 3602–3616, 2024, doi: 10.1177/14759217241276333.